Development/Plasticity/Repair

Effects of Cathodal Trans-Spinal Direct Current Stimulation on Mouse Spinal Network and Complex Multijoint Movements

Zaghloul Ahmed

Department of Physical Therapy, College of Staten Island for Developmental Neuroscience, the College of Staten Island, Staten Island, New York 10314, and Graduate Center/The City University of New York, New York, New York 10016

Cathodal trans-spinal direct current (c-tsDC) stimulation is a powerful technique to modulate spinal excitability. However, the manner in which c-tsDC stimulation modulates cortically evoked simple single-joint and complex multijoint movements is unknown. To address this issue, anesthetized mice were suspended with the hindlimb allowed to move freely in space. Simple and complex multijoint movements were elicited with short and prolonged trains of electrical stimulation, respectively, delivered to the area of primary motor cortex representing the hindlimb. In addition, spinal cord burst generators are known to be involved in a variety of motor activities, including locomotion, postural control, and voluntary movements. Therefore, to shed light into the mechanisms underlying movements modulated by c-tsDC stimulation, spinal circuit activity was induced using GABA and glycine receptor blockers, which produced three rates of spinal bursting activity: fast, intermediate, and slow. Characteristics of bursting activity were assessed during c-tsDC stimulation. During c-tsDC stimulation, significant increases were observed in (1) ankle dorsiflexion amplitude and speed; (2) ankle plantarflexion amplitude, speed, and duration; and (3) complex multijoint movement amplitude, speed, and duration. However, complex multijoint movement tracing showed that c-tsDC did not change the form of movements. In addition, spinal bursting activity was significantly modulated during c-tsDC stimulation: (1) fast bursting activity showed increased rate, amplitude, and duration; (2) intermediate bursting activity showed increased rate and duration, but decreased amplitude; and (3) slow bursting activity showed increased rate, but decreased duration and amplitude. These results suggest that c-tsDC stimulation amplifies cortically evoked movements through spinal mechanisms.

Introduction

Trans-spinal direct current (tsDC) stimulation is a neuromodulatory technique that causes immediate and long-term changes in spinal cord excitability (Aguilar et al., 2011; Ahmed, 2011, 2013; Cogiamanian et al., 2011; Truini et al., 2011; Ahmed and Wieraszko, 2012; Cogiamanian et al., 2012; Lamy et al., 2012; Lamy and Boakye, 2013). The overarching goal of tsDC stimulation is to restore function that has been lost due to spinal cord or brain injuries. Simple outcome measures, such as motor-evoked potentials, single muscle twitch, and H-reflex, have been used to evaluate the effects of tsDC stimulation on particular pathways. However, these measures do not elucidate how tsDC stimulation affects natural movements. Therefore, the current study investigated how cathodal tsDC (c-tsDC) stimulation modulates cortically elicited simple single-joint and complex multijoint movements.

Received July 1, 2013; revised Aug. 5, 2013; accepted Aug. 13, 2013.

Author contributions: Z.A. designed research; Z.A. performed research; Z.A. contributed unpublished reagents/analytic tools; Z.A. analyzed data; Z.A. wrote the paper.

This work was supported by Grant 64727-00 42 from Professional Staff Congress of the City University of New York.

Correspondence should be addressed to Zaghloul Ahmed at the above address. E-mail: zaghloul.ahmed@csi.cuny.edu.

DOI:10.1523/JNEUROSCI.2793-13.2013

 0270-6474/13/3314949-09$15.00/0

Spinal interneuronal networks known as central pattern generators (CPGs) are capable of generating rhythmic motor activity that activates limb muscles (Delcomyn, 1980; Grillner and Wallén, 1985). CPGs comprise smaller functional modules that can be combined in different patterns to produce a variety of motor activities (Grillner and Wallén, 1985; Kjaerulff and Kiehn, 1996; Grillner, 2006). Moreover, because spinal circuits are involved in transmission of voluntary movements (Prut and Perlmutter, 2003; Samara and Currie, 2008; Hart and Giszter, 2010; Roche et al., 2011; Bui et al., 2013), it seems reasonable to investigate whether c-tsDC stimulation influences spinal circuit activity.

When applied on the dorsum of the spinal cord, c-tsDC stimulation significantly enhances spinal excitability (Alanis, 1953; Eccles et al., 1962; Aguilar et al., 2011; Ahmed, 2011). This spinal facilitation can be exploited to restore motor or sensory function after brain or spinal cord injury. Indeed, combining c-tsDC with paired associative stimulation caused significant improvement in mice with unilateral spinal cord injury (Ahmed, 2013). Therefore, understanding how c-tsDC affects movement is of great clinical interest.

Mouse primary motor cortex (M1) contains maps for simple single-joint and complex multijoint movements that can be elicited by prolonged electrical microstimulation (Harrison et al., 2012). Stimulating M1 causes individual actions with kinematic

features (Raibert, 1977; Gordon and Ghez, 1987; Hening et al., 1988). In the present study, it was hypothesized that c-tsDC stimulation would affect the kinematics of M1-elicited movements and the bursting activity induced by blocking the spinal inhibitory system.

Epidural short and prolonged electrical stimulation of the hindlimb representation of M1 was used to produce simple single-joint and complex multijoint movements of the contralateral hindlimb. c-tsDC stimulation changed M1-induced movement kinematics by increasing movement size, duration, and speed. However, the movement form did not change. These findings indicate that although the brain may constrain movement form (Lacquaniti et al., 1983), the spinal cord plays a role in shaping movement kinematics. Spinal interneuron bursting activity was induced by blocking the inhibitory neurotransmitters glycine and GABA. Varying the concentration of the GABA blocker revealed three rates of synchronized bursting activity (fast, intermediate, slow), which were reliably recorded from the sciatic nerve and were significantly but differentially modulated by c-tsDC stimulation.

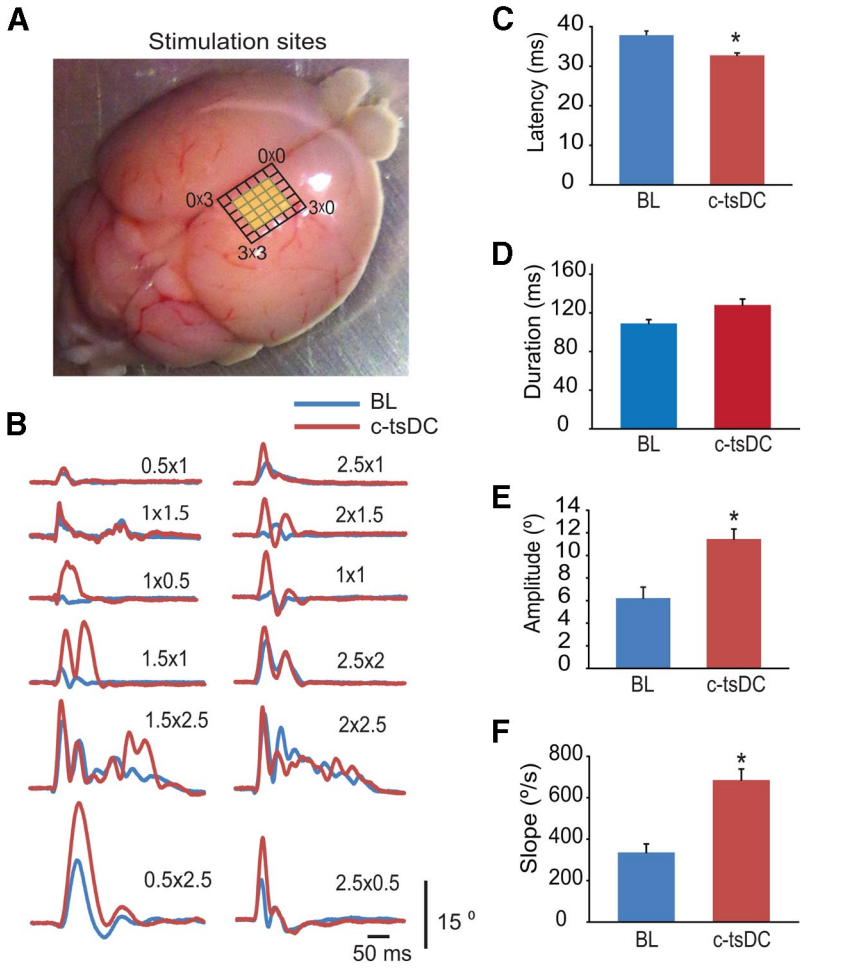

Figure 1. c-tsDC increased the amplitude of dorsiflexion movements. Movement traces were derived from an angle sensor. ***A***, Brain photograph showing sites of motor cortex where movements were elicited (yellow). ***B***, Dorsiflexion was elicited from 12 sites (lateral × posterior location relative to bregma labeled over traces). Note that c-tsDC stimulation increased dorsiflexion amplitude in all sites (red) compared with baseline (blue). Cortical stimulation intensity was 400 μA for sites 1.5 × 2.5 and 2 × 2.5 and 500 μA for all other sites. ***C***, Latency of dorsiflexion was significantly reduced during c-tsDC stimulation. ***D***, Movement duration was not changed during c-tsDC stimulation. ***E***, Dorsiflexion amplitude was significantly increased during c-tsDC stimulation. ***F***, Rising slope of the first deflection of the dorsiflexion movement was significantly increased during c-tsDC stimulation. *$p < 0.01$. Data are means ± SEM.

Materials and Methods

Animals. Adult male CD-1 mice ($n = 30$; weight, 35–40 g) were used for this study. Experiments were performed in accordance with the National Institutes of Health Guidelines for the Care and Use of Laboratory Animals. Protocols were approved by the Institutional Animal Care and Use Committee of the College of Staten Island. Animals were housed under a 12 h light/dark cycle with access to food and water *ad libitum*.

Procedure for movement-based measurements. Animals were anesthetized using ketamine/xylazine (90/10 mg/kg, i.p.). To elicit simple or complex multijoint movements, large craniotomies were performed to expose the two primary motor cortices for the hindlimbs (3 mm posterior and 3 mm lateral from bregma; Tennant et al., 2011). During this procedure, the dura remained intact and was kept moist with saline solution. The skin covering the thoracolumbar spinal region was dissected and moved to the side. Each animal was then placed in a suspension system (constructed in our laboratory), which supported the animal in prone position on a wooden dowel (1 cm thick) that was attached by Velcro to another wooden dowel at the top of the frame. A custom-designed holder was used to immobilize the head, and the four limbs were free to move in all directions.

The cortex was stimulated with a monopolar electrode (150 μm tip) situated on the dura covering the M1 area. Electrode placements were regularly spaced over 500 μm increments in a grid pattern, as shown in Figure 1*A* (Chakrabarty and Martin, 2000; Young et al., 2011). Sites of stimulation were located at grid intersections. The reference electrode was an alligator clip attached to a flap of scalp skin on the frontal aspect of the skull. Testing protocols started 20 min after injection of anesthetic. If needed, additional small anesthetic doses (5% of the first injection) were administered subcutaneously to produce gradual and therefore stable changes in the depth of anesthesia (Ahmed, 2013). The stimulation pulse was biphasic to minimize potential damage that could be induced by prolonged stimulation trains. Simple movements ($n = 5$) were elicited by short trains (60 ms) of seven pulses (0.3 ms duration; 100 Hz), and complex multijoint movements ($n = 10$) were elicited by prolonged trains (600 ms) of pulses (0.3 ms duration; 200 Hz). This extended duration of electrical stimulation was approximating the duration of a mouse stepping (Wooley et al., 2005) or scratching (McQueen et al., 2007). The selection of relatively higher current intensities was necessary to elicit movement due to the noninvasiveness of our procedure (i.e., electrodes placed on the surface of the dura). Specificity and latency of the responses strongly indicated that the source of the movement was confined to the stimulated region (see Results). This method was preferred to maintain the integrity of the cortical circuits and to minimize damage that could occur with prolonged trains, since the dura can protect the neural tissue. Stimulation was performed using a PowerLab stimulator and stimulus isolator unit (FE180, ADInstruments). At each cortical site, stimulation was gradually increased until multijoint movement was observed (~300 μA). The current was then increased to 600 μA, which induced near full-range multijoint movements. Complex multijoint movements were only observed in the hindlimb contralateral to M1, never in the ipsilateral hindlimb. In the procedure to elicit simple movement, the current was raised (maximal, 500 μA) until a clear twitch movement occurred either as plantarflexion or dorsiflexion.

A stainless steel electrode (50 μm thickness; 5 mm width; 10 mm length), covered with 2-mm-thick wick fabric, was used to deliver tsDC stimulation. The fabric side of the electrode was in contact with the body. This active electrode was placed over the vertebral column covering the lumbar enlargement area (Köbbert and Thanos, 2000; Watson et al., 2009). The reference electrode was an alligator clip attached to a flap of abdominal skin. A Grass S88X stimulator (Grass Technologies) in DC mode was used to generate tsDC, which was delivered through a stimulus-isolated unit (Grass Technologies). The present experiments used c-tsDC with an intensity of −0.8 mA and a duration of 8 s. Based on the area of the tsDC electrode, the current density at the electrode surface was 2.29 A/m^2, which is within the range considered safe (Liebetanz et al., 2009).

At each cortical site, baseline stimulation was first established to one stimulus with no c-tsDC, followed by one stimulus during c-tsDC, then another baseline stimulus with no c-tsDC. Site order for stimulation was randomized, and the cortical stimulation was identical before, during, and after c-tsDC stimulation. We did not observe any carryover effects of c-tsDC. Because data collected before and after c-tsDC were nearly identical, these data were averaged to be used as the baseline. Effects of c-tsDC were robust and reproducible across all animals and across all sites that evoked dorsiflexion, plantarflexion, or complex multijoint movements in the contralateral hindlimb. Thus, repetitive stimulation was not needed for confirmation. Although 25 sites were assayed, the complete procedure was conducted only at the sites that evoked simple or complex contralateral hindlimb movements.

To measure movements, a miniature flexible joint angle sensor (Measurand) was attached to the plantar aspect of the paw by double-sided adhesive tape. Multijoint complex movements were also videotaped using a standard camera, which was positioned to obtain a lateral view of the hindlimb, as shown in Figures 3*A* and 4*I*. Video recording was performed at 30 frames/s. Videos were exported to motion analysis software (MotionPro) to trace movement trajectory and to measure speed frame by frame.

Movement latency was measured as the time from the first pulse in the train to the time of movement onset, defined as the first deflection of the movement trace detected by the angle sensor. Movement duration was measured as the time from the onset of the movement to the end of the movement, defined as the time at which the trace value returned to baseline. Slope (°/s) was defined as the slope of a regression (least squares) line fitted to the data from 1–30% of the peak movement.

Procedure for spinal circuit measurements. Experiments measuring sciatic nerve synchrony and periodic bursting and their corresponding muscle forces were performed on anesthetized adult CD-1 mice ($n = 15$). Animals were placed in a mouse stereotaxic apparatus, which was placed in a custom-made clamping spinal column system. The bone at the base of the tail was fixed to the base of the system with surgical pins. Large bilateral laminectomies (T12-L4) were performed, and the sciatic nerve was cleared from the surrounding tissues. Both triceps surae (TS) and tibialis anterior (TA) muscles were carefully separated and their tendons connected to force transducers. Holes were made in the distal parts of the femur and tibia, and nails were inserted to fix these bones to the base. Sciatic nerve, TA muscle, and TS muscle were covered with a mixture of silicone oil and petroleum jelly (Vaseline). Muscle length was adjusted to allow maximal force.

Burst activity was induced by the injection of 5 μl of picrotoxin and strychnine mixture to the lumbar enlargement area. Injections were made using a Hamilton syringe (Neuros 10 μl) coupled with a 33 ga needle. Injection of the mixture was made at 0.7 mm below dura at four sites (1.25 μl/site, two on each side of the spinal cord, 2 mm apart). The injection sites corresponded approximately to the L5–L6 and L3–L4 junctions. All injections were done over a period of 2 min with the syringe left in place for an additional 1 min. The concentration of strychnine was kept constant at 0.3 μM. To produce activity with different bursting rates (Schmitt et al., 2004), picrotoxin was administered at three concentrations: 1, 0.5, and 0.3 mM. Animals started to show sign of bursting activity at 10–15 min following the end of injections. Testing of c-tsDC effects on bursting activity occurred during the first 10 min of stable and continuous bursting activity.

Electrophysiological recordings were made from the sciatic nerve using a hook electrode (80 μm diameter) that was coiled around the nerve trunk. A reference electrode was connected to the skin of the paw. The sciatic nerve was insulated from the underlying tissue with a thin silicone rubber sheet. Following injection of blockers, a stainless steel c-tsDC electrode covered with a wick fabric soaked with 0.9% saline was placed over the laminactomy area. The reference electrode was an alligator clip that was attached to a flap of abdominal skin. The intensity of c-tsDC stimulation was 0.8 mA in all experiments. The current was ramped up over 5 s, maintained for 30 s, and then ramped down over 5 s. Bursting activity during the constant 30 s stimulation period was compared with baseline activity during the 30 s before c-tsDC stimulation. Immediately following cessation of c-tsDC stimulation, bursting activity values returned to baseline values. There were no long-term effects of this protocol. Therefore, bursting activity following the cessation of c-tsDC stimulation was not considered for analysis. Extracellular activity was passed through a standard head stage, amplified (Neuro Amp EX, AD-Instruments), filtered (100 Hz–5 kHz bandpass), digitized at 4 kHz, and stored in the computer for further processing. A power laboratory data acquisition system and LabChart 7 software (ADInstruments) were used to acquire and analyze the data. Interburst interval (IBI) was measured as the time from the onset of one burst to the onset of the next, and onset was defined as the start of the rising phase of the response. Burst duration was the time from the onset of the burst to its end, defined at the first return to baseline values. Burst amplitude was calculated as the vertical distance measured in microvolts between the negative and positive peaks of the response.

Statistics. Data are graphed as means ± SEM. Paired *t* tests were used to compare baseline to c-tsDC for measurements of both movement and bursting activity. The differences between groups over time were assessed using repeated-measures ANOVA with a Holm–Sidak *post hoc* correction for testing differences between results at different time points (speed measurements). Statistical analyses were performed using SigmaPlot (SPSS). Autocorrelations were made using Spike Histogram Module in Labchart software (ADInstruments).

Results

Simple movements

Short-duration trains (60 ms) elicited simple ankle movements, such as dorsiflexion and plantarflexion. The location and direction of the movement was monitored visually and confirmed by angle sensor recording. Dorsiflexion was the most common movement observed in the contralateral hindlimb and was elicited from 12 sites of M1 in most animals (Fig. 1). Compared with baseline, during c-tsDC stimulation, latency of dorsiflexion was significantly reduced (37.8 ± 1.0 ms vs 32.8 ± 0.6 ms, $p < 0.01$, paired *t* test), amplitude was significantly increased (6.2 ± 1.0° vs 11.5 ± 0.9°, $p < 0.002$, paired *t* test), and rising slope of the first deflection of the movement was significantly increased (336.2 ± 40.9°/s vs 685.7 ± 52.9°/s, $p < 0.001$, paired *t* test). However, movement duration was not significantly changed (103.9 ± 3.8 ms vs 122.1 ± 5.9 ms, $p > 0.05$, paired *t* test).

Plantarflexion was less common and was elicited from only four sites of M1 (Fig. 2). Compared with baseline, during c-tsDC stimulation, movement amplitude was significantly increased (6.3 ± 1.1° vs 8.6 ± 2.2°, $p < 0.05$, paired *t* test), duration was significantly increased (125.3 ± 21.3 ms vs 143.3 ± 23.5 ms, $p < 0.05$, paired *t* test), and slope was significantly increased (211.6 ± 21.6°/s vs 271.5 ± 28.7°/s, $p < 0.05$, paired *t* test), but no changes were observed in latency (18.9 ± 0.5 ms vs 18.1 ± 0.3 ms, $p > 0.05$, paired *t* test).

To explore the effect of c-tsDC stimulation on different movement directions, percentage change values relative to baseline were compared between dorsiflexion and plantarflexion. Compared with plantarflexion, dorsiflexion showed significantly greater changes in latency (−14.8 ± 3.3% vs −4.1 ± 2.5%, $p <$

0.05, *t* test), amplitude (median 76.7 vs 22.9%, $p < 0.01$, Mann–Whitney test), and slope (median 130.1 vs 27.7%, $p < 0.05$, Mann–Whitney test), but not duration (20.2 ± 10.6% vs 12.4 ± 3.6%, $p > 0.05$, *t* test).

Next, the effect of electrode position was assessed. A significant effect of electrode position was found on the percentage change from baseline for the amplitude of dorsiflexion ($F = 5.7$; $p < 0.001$, one-way ANOVA). Specifically, three cortical sites showed significantly greater changes during c-tsDC: cortical site 1 × 1 showed greater changes than sites 2.5 × 1, 1 × 1.5, 2.5 × 0.5, and 2 × 2.5 ($p < 0.001$, Holm–Sidak method); 0.5 × 2.5 showed greater changes than 2 × 2.5 ($p < 0.01$, Holm–Sidak method); and 1.5 × 2.5 showed greater changes than 2 × 2.5 ($p \leq 0.01$, Holm–Sidak method). There was no effect of electrode position on percentage change from baseline for the amplitude of plantarflexion ($F = 2.5$; $p > 0.05$, one-way ANOVA).

Complex multijoint movements

Long-duration trains (600 ms) were used to elicit complex multijoint movements at the contralateral hindlimb (Fig. 3*A*). To compare the effects of c-tsDC stimulation to baseline, data composites from all sites were used. Relative to baseline, during c-tsDC, there were significant increases in amplitude (18.9 ± 2.6° vs 27.8 ± 2.7°, $p < 0.001$, paired *t* test), duration (median, 0.6 vs 0.7 s, $p < 0.01$, Wilcoxon signed-rank test), and slope (306.5 ± 56.8°/s vs 497.9 ± 54.8°/s, $p < 0.001$, paired *t* test), but no change in latency of movement onset (33.6 vs 34.9 ms, $p > 0.05$, paired *t* test; Fig. 3*B*). The data clearly revealed that c-tsDC stimulation increased the amplitude of complex multijoint movements elicited from all cortical sites (Fig. 3*D*,*E*), and electrode position had no significant effect on complex movements ($F = 0.14$, $p > 0.05$, one-way ANOVA).

The angle sensor did not reveal a complete picture of the changes in complex multijoint movements of the hindlimb. Therefore, in four animals, complex multijoint movements elicited by stimulating the central region of the hindlimb representation were videotaped and traced using a dot marked on the fifth digit, as shown in Figure 4. Relative to baseline, during c-tsDC, movement size and number of turns were affected, but general features, such as direction and final location in space, were unchanged. Traces from Animals 1–3 were elicited by stimulating the right cortex, 2 mm lateral and 1.5 pos-

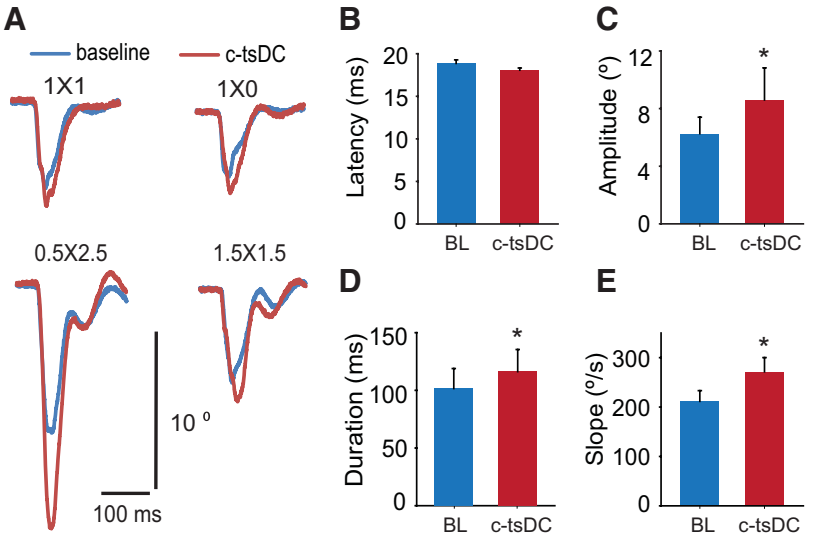

Figure 2. c-tsDC stimulation increased the amplitude of plantarflexion movements. Movement traces were derived from an angle sensor. Cortical stimulation was at 500 μA at all sites. ***A***, Plantarflexion was elicited from four sites (lateral × posterior location relative to bregma labeled over traces). ***B***, No significant change in movement latency was observed during c-tsDC stimulation. ***C***, Amplitude was significantly increased during c-tsDC stimulation. ***D***, Duration was significantly increased during c-tsDC stimulation. ***E***, Movement slope was significantly increased during c-tsDC stimulation. *$p < 0.01$. Data are means ± SEM.

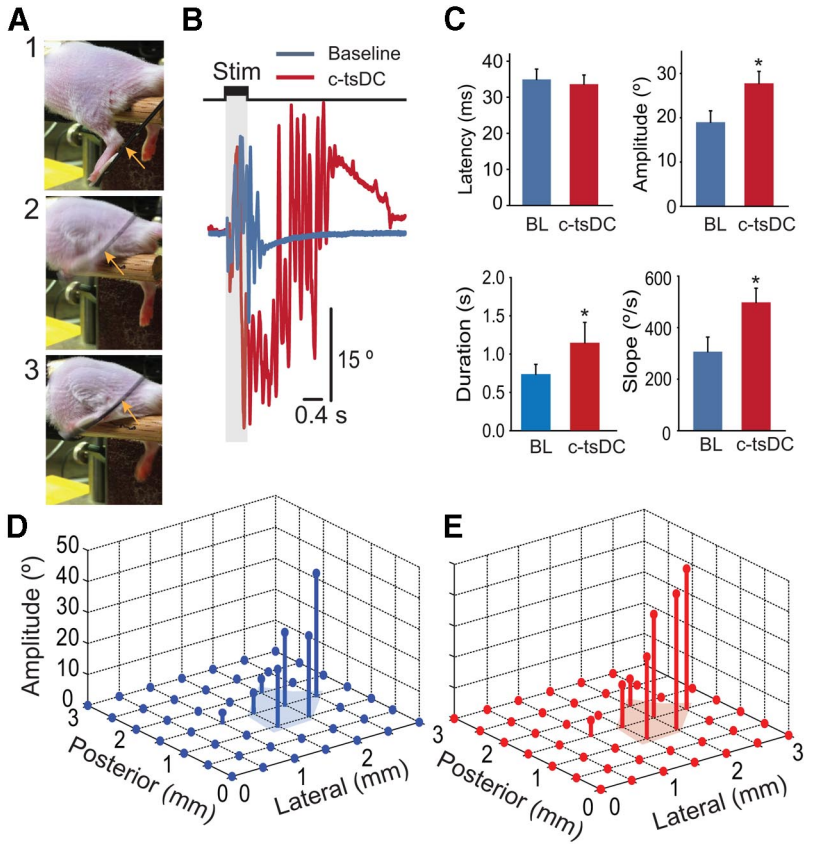

Figure 3. Effects of c-tsDC stimulation on complex multijoint movements of the hindlimb. Each animal was anesthetized, its head was restrained, and its body was supported with a system constructed at our laboratory that left the hindlimb free to move in all directions. Movement traces were derived from an angle sensor. ***A***, Three consecutive video frames: (***1***) before cortical stimulation, (***2***) just before holding position, and (***3***) at holding position. Arrows mark the angle sensor. ***B***, Examples of movement traces recorded with the angle sensor. The cortical stimulation time is shown at the top of the graph. Note that stimulation time (600 ms) is much shorter than the movement time, especially during c-tsDC stimulation (red). ***C***, Latency was unchanged, but amplitude, duration, and slope were increased by c-tsDC stimulation. *$p < 0.05$ ($n = 10$). ***D***, ***E***, Complex multijoint movement map based on amplitude measured by the angle sensor shows the average amplitude of the movements at baseline (***D***) and during c-tsDC stimulation (***E***; $n = 10$). Bregma is denoted by the 0.0 point, and the shaded region indicates the cortical area where stimulation evoked the greatest complex multijoint movement. Data are means ± SEM.

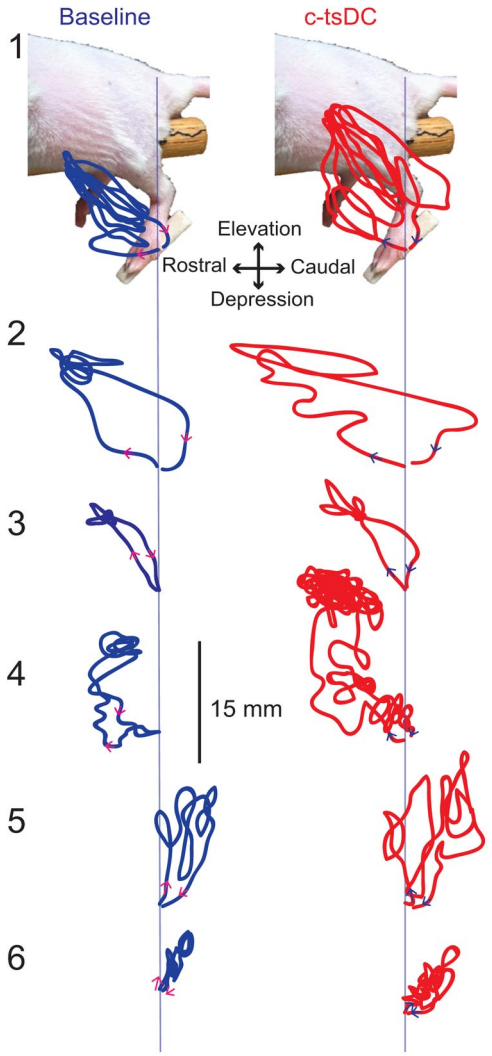

Figure 4. c-tsDC stimulation changed the amplitude of the movements but not their form. Movement traces were derived from video tracking (30 frames/s). Complex multijoint movements were elicited in four animals by stimulating the contralateral motor cortex; Traces 1–3 are from different animals, and Traces 4–6 are from the same animal. Trace 4 shows left hindlimb movement elicited by stimulating the right cortex, and Traces 5 and 6 show right hindlimb movement elicited by stimulating the left cortex at two different sites. Movements were videotaped, and the fifth digit was marked and traced using motion analysis software. Trace 1 is overlaid on a photograph of the animal. The vertical lines show the start and end of each movement.

terior from bregma. In Animal 1, the amplitude and number of turns were increased during c-tsDC stimulation. However, the general features of the movement were similar. In Animal 2, the amplitude was increased, but the number of turns at the peak of movement was reduced. In Animal 3, the amplitude changed, but the number of turns did not. In Animal 4, when the right cortex was stimulated 2 mm lateral and 1.5 mm posterior from bregma (Trace 4), both amplitude and number of turns were increased. However, the general pattern was not changed. In this same animal, when the left cortex was stimulated in two locations (Trace 5: 2 mm lateral and 1.5 posterior from bregma; Trace 6: 1.5 mm lateral and 1.5 posterior from bregma), right hindlimb movement was increased in size, but movement features did not change. These findings indicate that the general features of the movement were determined by the brain, but the size and other kinematics of the movement were determined locally by spinal circuits.

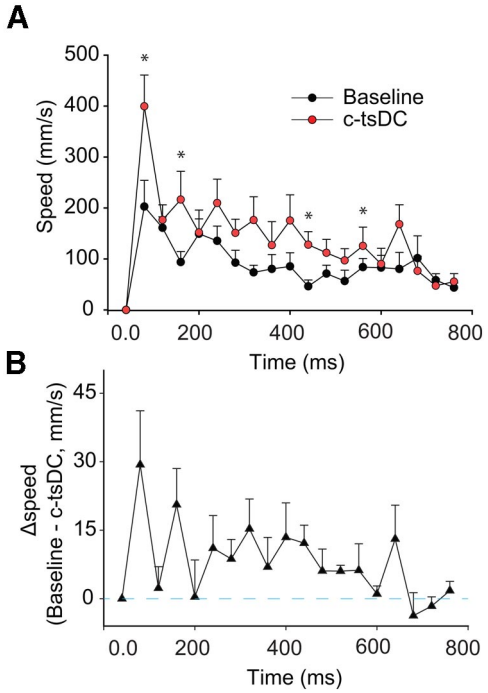

Figure 5. c-tsDC stimulation increased the speed of complex multijoint movements. Speed profiles are shown for the first 800 ms of the movements shown in Figure 4. ***A***, Speed was significantly increased at four points during c-tsDC stimulation. *$p < 0.05$, Holm–Sidak *post hoc* test. ***B***, Change in speed from baseline to c-tsDC stimulation. Data are means ± SEM.

Speed profiles of complex multijoint movements were calculated using motion analysis software. As shown in Figure 5, c-tsDC stimulation significantly increased the speed of the movements at four time points ($F = 8.7$, $p < 0.001$, repeated-measures ANOVA).

Effects of c-tsDC stimulation on spinal circuits

To test the effects of c-tsDC stimulation on spinal circuits, a mixture of picrotoxin and strychnine was injected into the lumber spinal cord to generate bursting electrical activity that could be recorded from the sciatic nerve. To determine the synchronicity of the bursts, muscle force was recorded from two antagonistic muscles, TA and TS. Depending on the concentration of the mixture, different firing patterns were produced. Bursting patterns were classified according to their IBI. Three patterns that were reproducible across animals were tested: fast, intermediate, and slow.

Fast bursting activity was defined as IBI of <200 ms (Fig. 6*A*). As shown in Figure 6*B*, relative to baseline, during c-tsDC, significant increases were observed in burst rate (decreased IBI; 170.3 ± 2.3 ms vs 148.7 ± 3.1 ms, $p < 0.001$, paired t test), duration (36.1 ± 1.1 ms vs 47.2 ± 2.9 ms, $p < 0.01$, paired t test), and amplitude (783.8 ± 45.6 μV vs 1753.9 ± 81.5 μV, $p < 0.001$, paired t test). TA and TS muscle force changes mirrored the changes in bursting electrical activity (Fig. 6*C*), and both muscles contracted at the same time, indicating that the bursting activity was synchronous. The average autocorrelation was calculated (Fig. 6*D*), revealing periodic patterns that indicate oscillations of ~7 Hz during c-tsDC stimulation, compared with ~5 Hz at baseline.

Intermediate bursting activity was defined as IBI >1 s but <2 s (Fig. 7*A*). As shown in Figure 7*B*, relative to baseline, during c-tsDC, significant increases were observed in burst rate (de-

creased IBI; 1.6 ± 0.1 s vs 1.2 ± 0.1 s, $p < 0.001$, paired t test) and duration (140.0 ± 6.4 ms vs 165.2 ± 7.3 ms, $p < 0.001$, paired t test), but amplitude was significantly reduced (1061.3 ± 54.8 μV vs 879.2 ± 62.6 μV, $p < 0.02$, paired t test). TA and TS muscle forces mirrored bursting electrical activity (Fig. 7*C*). The average autocorrelation (Fig. 7*D*) showed periodic patterns indicating oscillation during c-tsDC stimulation at ~0.83 Hz, compared with ~0.60 Hz at baseline. Moreover, during c-tsDC stimulation, bursting activity appeared more rhythmic (Fig. 7*D*).

Slow bursting activity was defined as IBI >5 s (Fig. 8*A*). As shown in Figure 8*B*, relative to baseline, during c-tsDC stimulation, significant increases were observed in burst rate (decreased IBI; 6.8 ± 0.5 s vs 2.7 ± 0.2 s, $p < 0.001$, paired t test), but significant reductions were observed in duration (2.8 ± 0.5 s vs 1.2 ± 0.1 s, $p < 0.02$, paired t test) and amplitude (603.8 ± 62.4 μV vs 323.8 ± 42.5 μV, $p < 0.02$, paired t test). TA and TS muscle forces mirrored bursting electrical activity (Fig. 7*C*). The average autocorrelation (Fig. 8*D*) showed periodic patterns indicating oscillation during c-tsDC stimulation at ~0.41 Hz, compared ~0.14 Hz at baseline. Collectively, these results indicate that c-tsDC stimulation has strong modulatory effects on the spinal network.

Discussion

This study demonstrated that c-tsDC stimulation modified simple single-joint and complex multijoint movements. Plantarflexion movements were increased in amplitude, duration, and slope, but not latency. This was most likely due to increased TS muscle force produced by c-tsDC stimulation (Ahmed, 2011; Ahmed and Wieraszko, 2012). Dorsiflexion movements showed decreased latency and increased amplitude and slope, but no change in duration. There was no change in the form of the dorsiflexion or plantarflexion movements.

It should be noted that dorsiflexion movements generally have longer latency than plantarflexion (~38 vs 18 ms), which could be due to cortical or spinal differences in how the two movements are produced. The shortening of movement latency during c-tsDC stimulation relates to faster processing at the level of spinal cord circuitry, which agrees with the findings that c-tsDC stimulation increases bursting rate (Figs. 6–8). Processing of movement initiation in the cortex (Isomura et al., 2009) could also be shortened

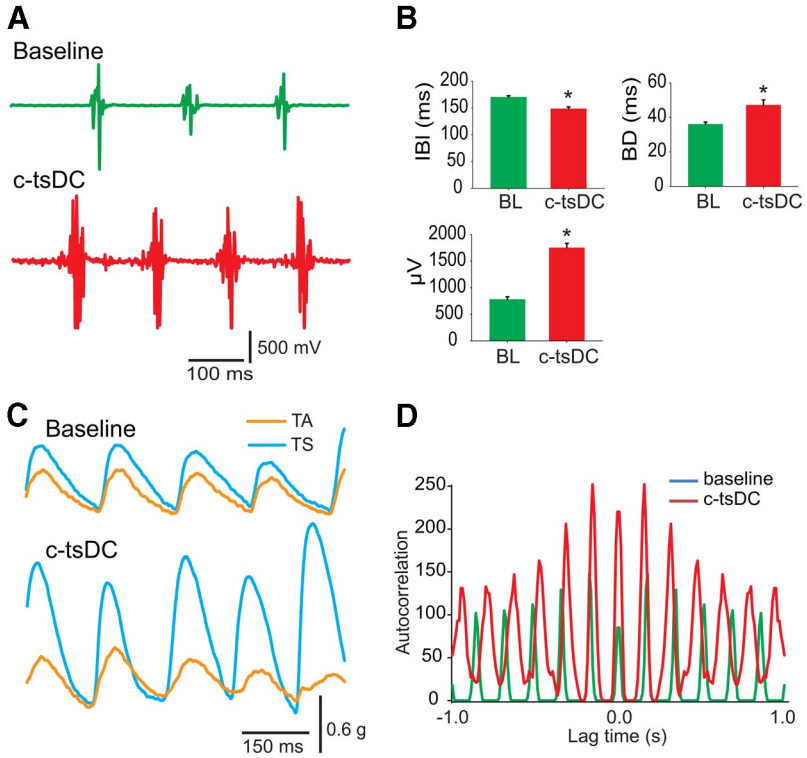

Figure 6. c-tsDC modulates fast bursting activity (IBI, <200 ms). ***A***, Examples of bursting activity recorded at baseline (green) and during c-tsDC (red). ***B***, Summary plots showing that c-tsDC significantly increased burst rate (reduced IBI), duration, and amplitude. ***C***, Muscle twitches from antagonistic TA and TS muscles recorded simultaneously show that the induced activity is synchronous and motor in nature. ***D***, Average autocorrelations calculated for baseline (green) and during c-tsDC (red). *$p < 0.05$. Data are means ± SEM.

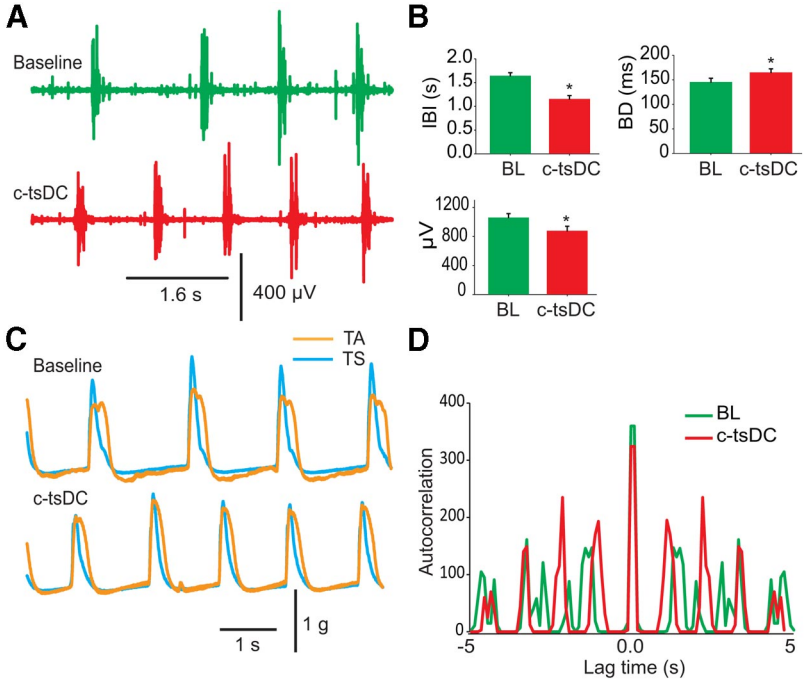

Figure 7. c-tsDC stimulation modulates intermediate bursting activity (IBI, >1 s but <2 s). ***A***, Examples of bursts recorded at baseline (green) and during c-tsDC stimulation (red). Note that there were four bursts during c-tsDC stimulation compared with three during baseline over the same recording period. ***B***, Summary plots showing that c-tsDC stimulation significantly increased burst rate (reduced IBI) and duration, but reduced amplitude. ***C***, Muscle twitch recorded simultaneously from TA and TS muscles. ***D***, Average autocorrelations calculated for baseline (green) and during c-tsDC stimulation (red) showed that burst activity became more rhythmic during c-tsDC stimulation. *$p < 0.05$. Data are means ± SEM.

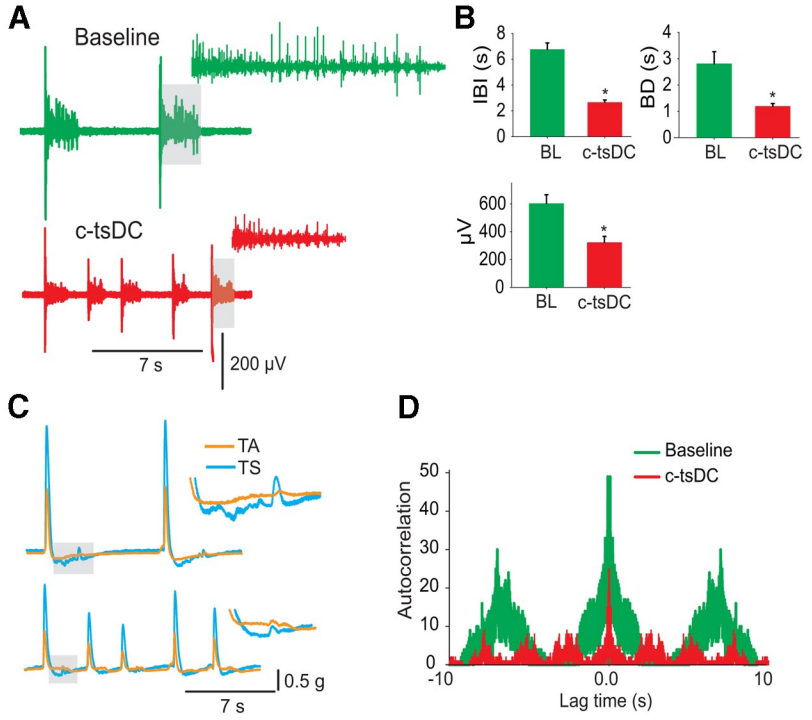

Figure 8. c-tsDC stimulation modulates slow bursting activity (IBI, >5 s). ***A***, Examples of slow burst activity at baseline (green) and during c-tsDC stimulation (red). These bursts contain sub-bursts, as shown in the expanded illustration. Expanded illustration corresponds to the shaded area. ***B***, Summary plots showing that c-tsDC stimulation significantly increased burst rate (reduced IBI), but reduced duration and amplitude. ***C***, Examples of muscle twitches recorded simultaneously from TA and TS muscles. The expanded area shows muscle twitches corresponding to the sub-bursts. ***D***, Average autocorrelations calculated for baseline (green) and during c-tsDC stimulation (red) showed clear changes in bursting activity during c-tsDC stimulation. $*p < 0.05$. Data are means ± SEM.

during c-tsDC stimulation by potentiated tonic sensory feedback (Aguilar et al., 2011). Increasing amplitude and slope of movements indicate that c-tsDC stimulation reconfigures spinal circuitry to recruit larger motor units (Ahmed and Wieraszko, 2012). This also relates to the finding that c-tsDC stimulation increased the amplitude of bursting activity (Fig. 6). c-tsDC stimulation induced changes in movement kinematics that were observed in movements elicited from all cortical sites. Analysis of electrode position showed that, in general, c-tsDC stimulation had similar effects on the majority of sites evoking dorsiflexion and on all sites evoking plantarflexion and complex multijoint movements. This suggests that c-tsDC activates a common spinal circuitry, albeit in different combinations, especially in the case of complex movement. However, c-tsDC stimulation differentially affected some sites that induced dorsiflexion, suggesting that different sites in M1 may produce the same movement (dorsiflexion) through different pathways.

Complex multijoint movements showed increased amplitude, duration, and slope, but not latency during c-tsDC stimulation. Complex multijoint movements elicited in the current study have behavioral relevance. For example, some of the evoked movements resembled voluntary scratching or stepping movements. The duration of the complex multijoint movement significantly outlasted the stimulus duration, sometimes by as long as 4 s (Fig. 3*B*), indicating that the stimulus served as a trigger to initiate movement. Movement duration was significantly prolonged during c-tsDC stimulation, which could be due to reverberating processes locally at the spinal cord or between the spinal cord and brain. Potentiated sensory feedback may be a mediating factor of this process. Stimulating the sciatic nerve and recording responses from M1 revealed that sensory feedback was potentiated during c-tsDC stimulation (data not shown).

There is direct evidence of functional integration between descending motor control pathways and spinal burst-generating circuits (Hart and Giszter, 2004, 2010; Drew et al., 2008). There is also evidence of electrophysiological and anatomical connections between the corticospinal system and spinal cord in cat (Futami et al., 1979; Shinoda et al., 1986; Li and Martin, 2002) and mouse (Steward et al., 2004; Ahmed, 2013). Fictive locomotion studies (Hamm et al., 1999) have shown that spinal cord circuits can generate activity patterns that drive single-joint or multijoint muscle synergies. The general idea is that CPGs (Grillner and Wallén, 1985) or spinal modules (Bizzi et al., 1991; Giszter et al., 1993) are the building blocks of motor behavior (Hart and Giszter, 2010) and can be activated by descending pathways from the motor cortex during voluntary (Bizzi and Cheung, 2013) or locomotor movements (Chvatal and Ting, 2012). In addition, Harrison et al. (2012) found that blocking synaptic transmission at the motor cortex impaired generation of complex movement. They concluded that complex movement requires intracortical synaptic transmission. These studies, together with the present data, suggest that both cortical and spinal mechanisms are required for emergence of complex movement phenomena (Georgopoulos et al., 1986; Wessberg et al., 2000).

The general organization of the motor map in mouse (Tennant et al., 2011) resembles those found in other species, such as rat (Donoghue and Wise, 1982; Kleim et al., 1998) and monkey (Nudo et al., 1996). The hindlimb representation in mice is bordered by representations of the trunk and tail (medially and caudally) and the forelimb (laterally and rostrally), and it occupies an area ~1 mm^2 (Tennant et al., 2011). In previous studies, directions of hindlimb movements were not described. In the present study, two simple single-joint movements were evoked from the motor cortex. As seen in Figures 1 and 2, multiple overlapping sites for plantarflexion and dorsiflexion were identified, and three times as many sites evoked dorsiflexion as plantarflexion, which may be related to functional differences. While there was no clear topography of the two movements relative to each other, there was a tendency for sites that evoked plantarflexion to be located rostrally to sites that evoked dorsiflexion. The failure to find clear movement topography may be due to the spatial resolution of the stimulation protocol used in the present study. Complex multijoint movements were concentrated in the hindlimb representation (Fig. 4*D*; Tennant et al., 2011). Parcellation of motor cortex into functionally distinct zones according to the direction of evoked movement has been described for the forelimb in monkeys (Graziano and Aflalo, 2007), rats (Bonazzi et al., 2013), and mice (Harrison et al., 2012). The present data are consistent with these findings: mouse hindlimb motor representation was parceled according to direction of movement, as shown in Figure 4 (*1–4* vs *5* and *6*).

One of the most striking findings in the present study was that movement traces have elements that remain constant regardless of increases in movement size and speed. This is clearly shown when the same cortical site can produce different movement forms in different animals (Fig. 4, Traces 1–3). Moreover, different sites in the same animal can produce different movement forms (Fig. 4, Traces 4–6). All movements maintained their trace signature during c-tsDC stimulation, regardless of increases in size, speed, and number of rotations. These findings support the theory that the cortex determines movement signature (Graziano and Aflalo, 2007), and the spinal cord modifies the size, speed, and duration. In Figure 4, Trace 4, the baseline and c-tsDC traces look similar, but the hindpaw remained at the maximal elevation point longer and completed more turns during c-tsDC stimulation. While it is difficult to pinpoint the exact mechanism underlying these changes, the bursting activity suggests that spinal circuitry is responsible. Bursts maintained their characteristic numbers of sub-bursts (one, two, and multiple sub-bursts in Figs. 6, 7, and 8, respectively), but increased their rate (decreased IBI). Bursts also maintained their shape (Fig. 8*A*). Collectively, different configurations of spinal circuits appear to be responsible for different aspects of movement (Hamm et al., 1999; Hart and Giszter, 2004; Chvatal and Ting, 2012). For example, only the fast bursting configuration (Fig. 6) showed increases in both rate and amplitude, which could mediate increased movement size. Intermediate and slow bursting configurations could mediate other movement details, such as number of turns.

Activation of the spinal GABAergic system has been shown to reduce the rate of bursting activity (Tegnér et al., 1993; Tegnér and Grillner, 2000; Schmitt et al., 2004). Conversely, c-tsDC stimulation increases the rate of burst activity. This suggests two possible underlying mechanisms of c-tsDC: (1) direct inhibition of the spinal GABAergic system, or (2) increased excitability of postsynaptic neurons, which overpowers the GABAergic system. Activation of the GABAergic system slows burst rate without changing burst quality, amplitude, or regularity (Schmitt et al., 2004). However, c-tsDC stimulation evoked more rhythmic burst activity and changed its amplitude and duration, suggesting broader effects on spinal circuits. Excitatory glutamatergic rhythmic-generating spinal neurons determine the speed of burst activity (Hägglund et al., 2010; Talpalar and Kiehn, 2010), based on the level of activation of iontropic glutamate receptors (Talpalar and Kiehn, 2010). We previously demonstrated that c-tsDC stimulation increases glutamate release at the spinal cord (Ahmed and Wieraszko, 2012). This increased glutamate release may mediate the increased burst activity rate.

This study has clinical as well as theoretical implications. Clinically, because spinal cord injury can cause significant changes in spinal circuits (Lu et al., 2008; Martinez et al., 2012), c-tsDC stimulation could be used to enhance spinal excitability to promote function. Because c-tsDC stimulation can amplify spinal responses to descending inputs to magnify natural movements, it enhances the capacity of the nervous system to produce purposeful movements, which is especially critical after injury. For example, after injury, a weak input that would be insufficient to produce movement could be enhanced by c-tsDC stimulation to permit movement, akin to using magnifying glasses to restore poor vision. Furthermore, the preservation of movement form during c-tsDC stimulation should facilitate its functional application by promoting purposeful movements without evoking unintended movements. However, the present study was conducted on healthy animals, and whether c-tsDC stimulation has similar functional effects in injured animals is unknown.

Although these experiments did not directly test motor control or motor learning theory, the theoretical implication of the current study is that the spinal cord has a significant role in shaping cortically elicited movement, which is revealed by c-tsDC stimulation. The results suggest that certain aspects of movement can be determined at the level of the spinal cord, including size, duration, and speed. For example, a tennis player could increase the arc and speed of his arm swing at the level of spinal cord circuitry without changing the motor commands at the level of motor cortex. That is, certain aspects of movement kinematics may be learned and stored within spinal cord circuitry. Future studies are needed to reveal the physiological changes underlying spinal cord excitability and whether these changes could be potentiated over time.

References

Aguilar J, Pulecchi F, Dilena R, Oliviero A, Priori A, Foffani G (2011) Spinal direct current stimulation (sDCS) modulates the activity of gracile nucleus and primary somatosensory cortex in anesthetized rats. J Physiol 589:4981–4996. CrossRef Medline

Ahmed Z (2011) Trans-spinal direct current stimulation modulates motor cortex-induced muscle contraction in mice. J Appl Physiol 110:1414–1424. CrossRef Medline

Ahmed Z (2013) Electrophysiological characterization of spino-sciatic and cortico-sciatic associative plasticity: modulation by trans-spinal direct current and effects on recovery after spinal cord injury in mice. J Neurosci 33:4935–4946. CrossRef Medline

Ahmed Z, Wieraszko A (2012) Trans-spinal direct current enhances corticospinal output and stimulation-evoked release of 2 glutamate analog, D-2,33H-aspartic acid. J Appl Physiol 112:1576–1592. CrossRef Medline

Alanis J (1953) Effects of direct current on motor neurones. J Physiol 120:569–578. Medline

Bizzi E, Cheung VC (2013) The neural origin of muscle synergies. Front Comput Neurosci 7:51. Medline

Bizzi E, Mussa-Ivaldi FA, Giszter S (1991) Computations underlying the execution of movement: a biological perspective. Science 253:287–291. CrossRef Medline

Bonazzi L, Viaro R, Lodi E, Canto R, Bonifazzi C, Franchi G (2013) Complex movement topography and extrinsic space representation in the rat forelimb motor cortex as defined by long-duration intracortical microstimulation. J Neurosci 33:2097–2107. CrossRef Medline

Bui TV, Akay T, Loubani O, Hnasko TS, Jessell TM, Brownstone RM (2013) Circuits for grasping: spinal dI3 interneurons mediate cutaneous control of motor behavior. Neuron 78:191–204. CrossRef Medline

Chakrabarty S, Martin JH (2000) Postnatal development of the motor representation in primary motor cortex. J Neurophysiol 84:2582–2594. Medline

Chvatal SA, Ting LH (2012) Voluntary and reactive recruitment of locomotor muscle synergies during perturbed walking. J Neurosci 32:12237–12250. CrossRef Medline

Cogiamanian F, Vergari M, Schiaffi E, Marceglia S, Ardolino G, Barbieri S, Priori A (2011) Transcutaneous spinal cord direct current stimulation inhibits the lower limb nociceptive flexion reflex in human beings. Pain 152:370–375. CrossRef Medline

Cogiamanian F, Ardolino G, Vergari M, Ferrucci R, Ciocca M, Scelzo E, Barbieri S, Priori A (2012) Transcutaneous spinal direct current stimulation. Front Psychiatry 3:63. CrossRef Medline

Delcomyn F (1980) Neural basis of rhythmic behavior in animals. Science 210:492–498. CrossRef Medline

Donoghue JP, Wise SP (1982) The motor cortex of the rat: cytoarchitecture and microstimulation mapping. J Comp Neurol 212:76–88. CrossRef Medline

Drew T, Kalaska J, Krouchev N (2008) Muscle synergies during locomotion in the cat: a model for motor cortex control. J Physiol 586:1239–1245. CrossRef Medline

Eccles JC, Kostyuk PG, Schmidt RF (1962) The effect of electric polarization of the spinal cord on central afferent fibres and on their excitatory synaptic action. J Physiol 162:138–150. Medline

Futami T, Shinoda Y, Yokota J (1979) Spinal axon collaterals of corticospi-

nal neurons identified by intracellular injection of horseradish peroxidase. Brain Res 164:279–284. CrossRef Medline
Georgopoulos AP, Schwartz AB, Kettner RE (1986) Neuronal population coding of movement direction. Science 233:1416–1419. CrossRef Medline
Giszter SF, Mussa-Ivaldi FA, Bizzi E (1993) Convergent force fields organized in the frog's spinal cord. J Neurosci 13:467–491. Medline
Gordon J, Ghez C (1987) Trajectory control in targeted force impulses. II. Pulse height control. Exp Brain Res 67:241–252. CrossRef Medline
Graziano MS, Aflalo TN (2007) Mapping behavioral repertoire onto the cortex. Neuron 56:239–251. CrossRef Medline
Grillner S (2006) Biological pattern generation: the cellular and computational logic of networks in motion. Neuron 52:751–766. CrossRef Medline
Grillner S, Wallén P (1985) Central pattern generators for locomotion, with special reference to vertebrates. Annu Rev Neurosci 8:233–261. CrossRef Medline
Hägglund M, Borgius L, Dougherty KJ, Kiehn O (2010) Activation of groups of excitatory neurons in the mammalian spinal cord or hindbrain evokes locomotion. Nat Neurosci 13:246–252. CrossRef Medline
Hamm TM, Trank TV, Turkin VV (1999) Correlations between neurograms and locomotor drive potentials in motoneurons during fictive locomotion: implications for the organization of locomotor commands. Prog Brain Res 123:331–339. CrossRef Medline
Harrison TC, Ayling OG, Murphy TH (2012) Distinct cortical circuit mechanisms for complex forelimb movement and motor map topography. Neuron 74:397–409. CrossRef Medline
Hart CB, Giszter SF (2004) Modular premotor drives and unit bursts as primitives for frog motor behaviors. J Neurosci 24:5269–5282. CrossRef Medline
Hart CB, Giszter SF (2010) A neural basis for motor primitives in the spinal cord. J Neurosci 30:1322–1336. CrossRef Medline
Hening W, Vicario D, Ghez C (1988) Trajectory control in targeted force impulses. IV. Influences of choice, prior experience and urgency. Exp Brain Res 71:103–115. CrossRef Medline
Isomura Y, Harukuni R, Takekawa T, Aizawa H, Fukai T (2009) Microcircuitry coordination of cortical motor information in self-initiation of voluntary movements. Nat Neurosci 12:1586–1593. CrossRef Medline
Kjaerulff O, Kiehn O (1996) Distribution of networks generating and coordinating locomotor activity in the neonatal rat spinal cord *in vitro*: a lesion study. J Neurosci 16:5777–5794. Medline
Kleim JA, Barbay S, Nudo RJ (1998) Functional reorganization of the rat motor cortex following motor skill learning. J Neurophysiol 80:3321–3325. Medline
Köbbert C, Thanos S (2000) Topographic representation of the sciatic nerve motor neurons in the spinal cord of the adult rat correlates to region-specific activation patterns of microglia. J Neurocytol 29:271–283. CrossRef Medline
Lacquaniti F, Terzuolo C, Viviani P (1983) The law relating the kinematic and figural aspects of drawing movements. Acta Psychol (Amst) 54:115–130. CrossRef Medline
Lamy JC, Boakye M (2013) BDNF Val66Met polymorphism alters spinal DC stimulation-induced plasticity in humans. J Neurophysiol 110:109–116. CrossRef Medline
Lamy JC, Ho C, Badel A, Arrigo RT, Boakye M (2012) Modulation of soleus H reflex by spinal DC stimulation in humans. J Neurophysiol 108:906–914. CrossRef Medline
Li Q, Martin JH (2002) Postnatal development of connectional specificity of corticospinal terminals in the cat. J Comp Neurol 447:57–71. CrossRef Medline
Liebetanz D, Koch R, Mayenfels S, König F, Paulus W, Nitsche MA (2009) Safety limits of cathodal transcranial direct current stimulation in rats. Clin Neurophysiol 120:1161–1167. CrossRef Medline
Lu Y, Zheng J, Xiong L, Zimmermann M, Yang J (2008) Spinal cord injury-induced attenuation of GABAergic inhibition in spinal dorsal horn circuits is associated with down-regulation of the chloride transporter KCC2 in rat. J Physiol 586:5701–5715. CrossRef Medline
Martinez M, Delivet-Mongrain H, Leblond H, Rossignol S (2012) Incomplete spinal cord injury promotes durable functional changes within the spinal locomotor circuitry. J Neurophysiol 108:124–134. CrossRef Medline
McQueen DS, Noble MA, Bond SM (2007) Endothelin-1 activates ETA receptors to cause reflex scratching in BALB/c mice. Br J Pharmacol 151:278–284. CrossRef Medline
Nudo RJ, Milliken GW, Jenkins WM, Merzenich MM (1996) Use-dependent alterations of movement representations in primary motor cortex of adult squirrel monkeys. J Neurosci 16:785–807. Medline
Prut Y, Perlmutter SI (2003) Firing properties of spinal interneurons during voluntary movement. I. State-dependent regularity of firing. J Neurosci 23:9600–9610. Medline
Raibert MH (1977) Motor control and learning by the state-space model. Cambridge, MA: Artificial Intelligence Laboratory, Massachusetts Institute of Technology.
Roche N, Bussel B, Maier MA, Katz R, Lindberg P (2011) Impact of precision grip tasks on cervical spinal network excitability in humans. J Physiol 589:3545–3558. CrossRef Medline
Samara RF, Currie SN (2008) Location of spinal cord pathways that control hindlimb movement amplitude and interlimb coordination during voluntary swimming in turtles. J Neurophysiol 99:1953–1968. CrossRef Medline
Schmitt DE, Hill RH, Grillner S (2004) The spinal GABAergic system is a strong modulator of burst frequency in the lamprey locomotor network. J Neurophysiol 92:2357–2367. CrossRef Medline
Shinoda Y, Yamaguchi T, Futami T (1986) Multiple axon collaterals of single corticospinal axons in the cat spinal cord. J Neurophysiol 55:425–448. Medline
Steward O, Zheng B, Ho C, Anderson K, Tessier-Lavigne M (2004) The dorsolateral corticospinal tract in mice: an alternative route for corticospinal input to caudal segments following dorsal column lesions. J Comp Neurol 472:463–477. CrossRef Medline
Talpalar AE, Kiehn O (2010) Glutamatergic mechanisms for speed control and network operation in the rodent locomotor CpG. Front Neural Circuits 4:pii19. CrossRef Medline
Tegnér J, Grillner S (2000) GABA(B)-ergic modulation of burst rate and intersegmental coordination in lamprey: experiments and simulations. Brain Res 864:81–86. CrossRef Medline
Tegnér J, Matsushima T, el Manira A, Grillner S (1993) The spinal GABA system modulates burst frequency and intersegmental coordination in the lamprey: differential effects of GABAA and GABAB receptors. J Neurophysiol 69:647–657. Medline
Tennant KA, Adkins DL, Donlan NA, Asay AL, Thomas N, Kleim JA, Jones TA (2011) The organization of the forelimb representation of the C57BL/6 mouse motor cortex as defined by intracortical microstimulation and cytoarchitecture. Cereb Cortex 21:865–876. CrossRef Medline
Truini A, Vergari M, Biasiotta A, La Cesa S, Gabriele M, Di Stefano G, Cambieri C, Cruccu G, Inghilleri M, Priori A (2011) Transcutaneous spinal direct current stimulation inhibits nociceptive spinal pathway conduction and increases pain tolerance in humans. Eur J Pain 15:1023–1027. CrossRef Medline
Watson C, Paxinos G, Kayalioglu G, Heise C (2009) Atlas of the mouse spinal cord. In: The spinal cord (Watson C, Paxinos G, Kayalioglu G, eds), pp 308–379. San Diego: Academic.
Wessberg J, Stambaugh CR, Kralik JD, Beck PD, Laubach M, Chapin JK, Kim J, Biggs SJ, Srinivasan MA, Nicolelis MA (2000) Real-time prediction of hand trajectory by ensembles of cortical neurons in primates. Nature 408:361–365. CrossRef Medline
Wooley CM, Sher RB, Kale A, Frankel WN, Cox GA, Seburn KL (2005) Gait analysis detects early changes in transgenic SOD1(G93A) mice. Muscle Nerve 32:43–50. CrossRef Medline
Young NA, Vuong J, Flynn C, Teskey GC (2011) Optimal parameters for microstimulation derived forelimb movement thresholds and motor maps in rats and mice. J Neurosci Methods 196:60–69. CrossRef Medline